

# Estimation of topsoil moisture and hydraulic conductivity using infrared thermography in the Brazilian semiarid

*Estimativa da umidade e condutividade hidráulica do solo superficial usando termografia por infravermelhos no semiárido brasileiro*

Abelardo Antônio de Assunção Montenegro<sup>1</sup> , Valdemir de Paula e Silva Junior<sup>1</sup> ,  
João Luis Mendes Pedroso de Lima<sup>2\*</sup> , José Roberto Lopes da Silva<sup>1</sup> ,  
João Rafael Cardoso de Brito Abrantes<sup>3,4</sup> 

## ABSTRACT

This study introduces an exploratory technique for soil moisture and unsaturated hydraulic conductivity estimation, using infrared thermography. The technique consists in applying a certain volume of water to the soil surface and registering the temperature with an infrared camera. The applied water should have a lower or higher temperature than the soil surface in order to create a temperature gradient at the soil surface. Experiments were conducted in the Mimoso catchment, which is located in the semiarid region of the Brazilian state of Pernambuco, in two soils: Yellow Argisol and Fluvisol Neossol. Experiments were conducted at two distinct periods of the day: in the morning with cooler soil surface and in the afternoon with hooter soil surface. Different volumes of water were applied to the soil surface originating different soil moisture. Water was applied at two distinct temperatures of 10 - 15 and 80 - 85°C, according to the initial soil surface temperature. The technique allowed us to map estimated soil moisture with values obtained with infrared thermography. When compared with soil sampling, a correlation coefficient higher than 0.70 was observed. Based on the data obtained, it was possible to estimate the topsoil unsaturated soil hydraulic conductivity, relevant to the analysis of hydrological processes, such as infiltration.

**Keywords:** soil moisture; unsaturated hydraulic conductivity; field assessment; infrared thermography.

## RESUMO

Este estudo apresenta uma técnica exploratória para estimativa da umidade e da condutividade hidráulica não saturada da camada superficial do solo, utilizando a termografia por infravermelhos. A técnica consiste em aplicar um determinado volume de água na superfície do solo e registrar a temperatura com uma câmara de infravermelhos. A água aplicada deve ter temperatura inferior ou superior à superfície do solo, para criar um gradiente de temperatura na superfície do solo. Os experimentos foram conduzidos na bacia do Mimoso, localizada no semiárido do estado brasileiro de Pernambuco (Brasil), em dois solos: Argissolo Amarelo e Neossolo Flúvico. Os experimentos foram conduzidos em dois períodos distintos do dia: de manhã com do a superfície solo menos quente e à tarde com solo muito elevada. Diferentes volumes de água foram aplicados na superfície do solo originando distintas umidades do solo. A água foi aplicada com duas temperaturas distintas de 10 - 15 e 80 - 85°C, de acordo com a temperatura inicial da superfície do solo. A técnica permitiu mapear a umidade estimada do solo com valores obtidos com termografia de infravermelhos; quando comparado com amostragem de solo observaram-se coeficientes de correlação superior a 0,70. Com base nos dados obtidos, foi possível estimar a condutividade hidráulica da camada superficial do solo não saturado, relevante para a análise de processos hidrológicos, como a infiltração.

**Palavras-chave:** umidade do solo; condutividade hidráulica não saturada; avaliação de campo; termografia por infravermelhos.

<sup>1</sup>Universidade Federal Rural de Pernambuco - Recife (PE), Brazil.

<sup>2</sup>Universidade de Coimbra, Department of Civil Engineering, Faculty of Sciences and Technology, Marine and Environmental Sciences Centre, Aquatic Research Network - Coimbra, Portugal.

<sup>3</sup>Universidade de Coimbra, Civil Engineering Research and Innovation for Sustainability Research Unit - Coimbra, Portugal.

<sup>4</sup>Instituto de Investigação e Desenvolvimento Tecnológico para a Construção, Energia, Ambiente e Sustentabilidade - Coimbra, Portugal.

\*Corresponding author: plima@dec.ucp

**Conflicts of interest:** the authors declare no conflicts of interest.

**Funding:** To CAPES, Brazil, for the Doctoral grants of the second author (Fellowship 11526/13-0) and fourth author (Fellowship 1172340), and to CNPq, Brazil, for the Doctoral grants also of the fourth authors (Fellowship 370597/2011-7). To the FCT, Portugal, for the Doctoral grant SFRH/BD/103300/2014 of the fifth author. To CNPq, Brazil, for the financial support of the scholarship program of Special Visiting Researcher of the Brazilian scientific mobility program 'Science Without Borders', of the third author and the Universal Project of the first author. To FINEP, Brazil, for the financial support to the REHIDRO network.

**Received on:** 05/09/2023 - **Accepted on:** 07/28/2023

## INTRODUCTION

Soil hydraulic conductivity describes how easily water can move through the soil, which is extremely important for agriculture management and, consequently, to soil and environmental preservation (HURTADO; CICHOTA; LIER, 2005; GONÇALVES; LIBARDI, 2013). Bagarello *et al.* (2010) pointed out that soil hydraulic conductivity, soil density, and soil moisture are the most significant variables to be monitored in a river basin.

Soil hydraulic conductivity can be estimated both in the laboratory and *in situ*, the first being inconvenient due to the use of unrepresentative samples, reduced sampling dimensions, and the risk of damaging the soil structure (SILVA *et al.*, 2012, 2014). Carvalho *et al.* (2007) highlighted that determining hydraulic conductivity *in situ* is more precise than determining it in the laboratory. Bagarello *et al.* (2012) adopted an *in situ* infiltration experiment for the soil hydraulic characterization using the Beerkan method. This simplified methodology is also known as the simplified method based on a Beerkan Infiltration (BRAUD *et al.*, 2005; LASSABATÈRE *et al.*, 2006; BAGARELLO *et al.*, 2012). According to the authors, this method combines a physically based infiltration model (LASSABATÈRE *et al.*, 2006) with basic relationships between soil variables (REYNOLDS; ELRICK, 2002a, 2002b).

Infrared thermography-based methods have been used as high-resolution imaging tools in hydrology. Infrared thermography is a versatile, accurate, and fast technique of monitoring surface temperature and has been successfully employed as a high spatial and temporal resolution non-invasive and non-destructive imaging tool to access groundwater discharges into estuaries (MEJÍAS *et al.*, 2012) and streams (CHEN *et al.*, 2009), quantify thermal heterogeneity of streams (BONAR; PETRE, 2015) and floodplains (TONOLLA *et al.*, 2010), and map saturated area connectivity and dynamics (PFISTER *et al.*, 2010). Combining thermal imaging with the injection of hot water, as an artificial tracer technique, Schuetz *et al.* (2012) characterized the spatial distribution of flow paths and assessed flow transport properties. Voortman *et al.* (2016) assessed the representativeness of lysimeter

measurements with the aid of thermal imaging. In particular, studies using portable hand-held infrared cameras have been increasing due to recent reductions in their prices and substantial enhancements in their portability and spatial resolution.

In recent studies, infrared thermographic techniques were used by the authors to assess different soil surface hydrological processes both in laboratory (ABRANTES *et al.*, 2017, 2018; DE LIMA; ABRANTES, 2014a, 2014b; DE LIMA *et al.*, 2014, 2015a, 2015b; MUJTABA; DE LIMA, 2018) and field conditions (ABRANTES *et al.*, 2019; DE LIMA *et al.*, 2015b). In combination with thermal tracers, infrared thermography has also been applied in flow velocity measurements (ABRANTES *et al.*, 2019; DE LIMA; ABRANTES, 2014b; DE LIMA *et al.*, 2015b, 2021).

This study, based on fieldwork, aimed to evaluate the performance of a thermographic technique to help in mapping soil moisture and unsaturated hydraulic conductivity of the topsoil of two dominant soils (Yellow Argisol and a Fluvisol Neossol) in the Mimoso catchment located in the semiarid area of the Pernambuco state, Brazil. This study is a follow-up of exploratory laboratory tests presented by de Lima *et al.* (2014b), where an infrared thermography technique was used to identify preferential flux of water into the soil and map areas of the soil surface with higher and lower permeability.

## MATERIAL AND METHODS

### Study site

Experiments were developed at the Mimoso catchment (located within the coordinates 8° 34' 17" – 8° 11" S and 37° 1' 35" – 36° 47' 20" W), part of the Alto Ipanema catchment located in the Brazilian semiarid region of Pernambuco State (Figure 1). With an area of 124 km<sup>2</sup>, the Mimoso catchment consists essentially of non-perennial streams and has been monitored as part of the REHISA network ("Rede de Hidrologia do Semiárido," Brazil). Soils with a thickness of

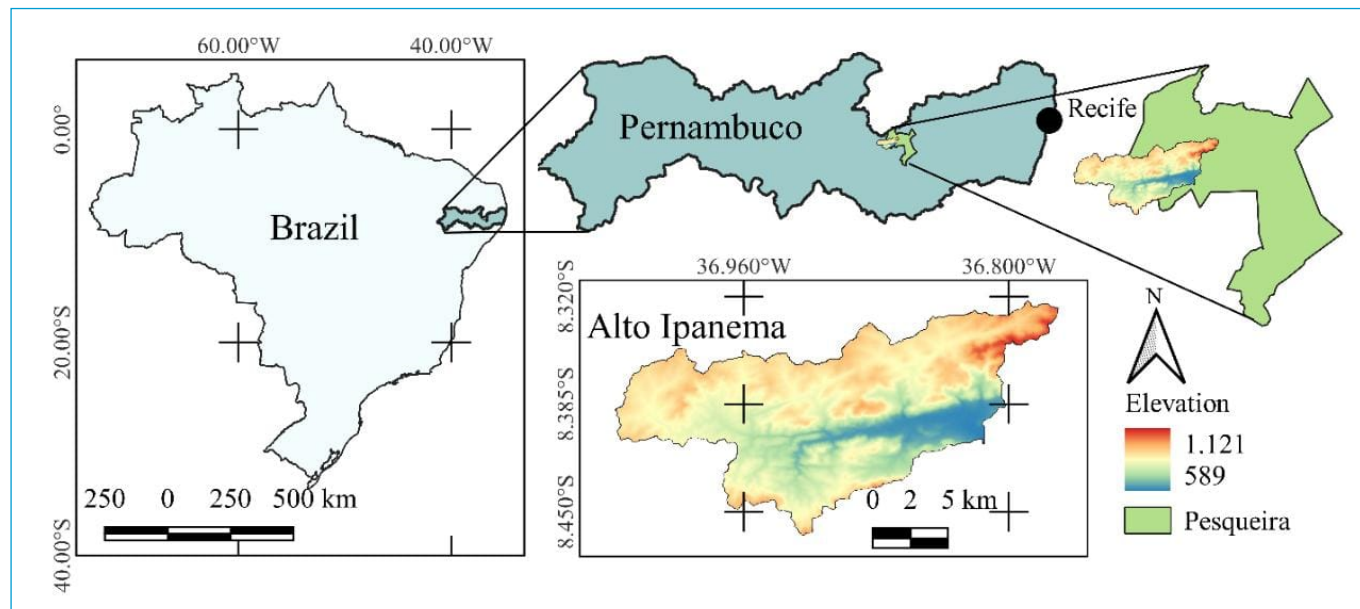


Figure 1 – Location of the Alto Ipanema Basin in the State of Pernambuco, Brazil.

less than 2 m at the hillslopes are dominant. Communal rainfed agriculture is developed in these hillslopes, usually without appropriate management, due to poor incomes and small properties.

The thermographic technique was tested in two distinct soil types: a Yellow Argisol and a Fluvic Neossol. Yellow Argisol presented 29.6% sand, 34.0% clay, and 36.4% silt with a natural bulk density of  $\sim 1,700 \text{ kg m}^{-3}$ . Fluvic Neossol presented 67.0% sand, 14.8% clay, and 18.2% silt with a natural bulk density of  $\sim 1,400 \text{ kg m}^{-3}$ . In the field, experiments were conducted on flat terrains in bare soils (Figure 2).

Experiments were conducted in two distinct periods of the day: in the morning ( $\sim 7 \text{ a.m.}$ ) and in the afternoon ( $\sim 3 \text{ p.m.}$ ). In the afternoon period, experiments were conducted considering two distinct locations: a cooler area under the tree canopy and a hotter area under direct sunlight. This allowed testing the thermographic technique in three distinct initial soil surface temperatures: cooler soil surface at an average temperature of  $34.0 \pm 3.0^\circ\text{C}$  in the early morning approximately 2 h after sunrise, hot soil surface during the afternoon, at average temperatures of  $50.4 \pm 3.1$  and  $65.8 \pm 2.4^\circ\text{C}$  under the tree canopy and direct sunlight, respectively. Volumetric soil moisture, measured through soil sampling (following the prescribed in EMBRAPA, 1997) of the two soils at the beginning of the experiments was  $5.0 \pm 0.3\%$  in the morning period and  $1.0 \pm 0.1\%$  in the afternoon period.

Mean atmospheric conditions were recorded with a Campbell Scientific MetPRO Model Automatic Station, with rain gauge, anemometer, pyranometer, air temperature, and air humidity sensors.

During the fieldwork, mean air temperature was  $26.1^\circ\text{C}$ , relative humidity was 58.9%, wind velocity was  $3.3 \text{ m}\cdot\text{s}$ , and solar radiation was  $41.1 \text{ MJ}\cdot\text{m}^2$ .

## Experimental procedure

The thermographic technique consists in applying a certain amount of water on the soil surface, in rings, and registering the soil surface temperature to estimate soil moisture and unsaturated hydraulic conductivity

of the topsoil layer. The applied water should have a lower or higher temperature than the soil surface in order to create a temperature gradient at the soil surface.

Polyvinyl chloride (PVC) rings (Figure 2), with a diameter of 0.2 m, were installed and inserted in the soil to a depth of approximately 0.15 m in order to avoid lateral loss of water. The delimiting rings were inserted at a distance of 0.4 – 0.5 m from each other. Four different volumes of water were applied to the soil surface: 100, 150, 200, and 250 mL, producing an initial water depth of 3.2, 4.8, 6.4, and 8.0 mm, respectively, inside the PVC rings. Water was applied at two distinct temperatures, according to the initial soil surface temperature: hot water at  $80 - 85^\circ\text{C}$  in the experiments conducted during the morning and cold water at  $10 - 15^\circ\text{C}$  in the experiments conducted during the afternoon. These allowed temperature differences between the water and the soil surface of approximately  $50^\circ\text{C}$  for the morning experiments and 40 and  $55^\circ\text{C}$  for the afternoon experiments.

Thermal images of the soil surface temperature distribution were registered every 5 min after the water application, using an infrared camera (Model E6 from Flir Systems) with a spatial resolution of  $120 \times 160$  pixels, positioned 0.5 m above the soil surface. For each soil type, a total of 72 soil surface thermograms were registered and analyzed: three repetitions for each of the four applied water volumes with two experiments conducted during the morning period (colder soil and hotter water) and four experiments conducted during the afternoon period (warmer soil and colder water).

Samples of the soil after application of the water volumes were collected to a depth of 0.05 m inside the PVC rings, immediately after the registration of the soil surface temperature with the infrared camera, in order to determine volumetric soil moisture (EMBRAPA, 1997).

## Data analyses

The thermal images registered with the infrared camera were analyzed with the objective of identifying differences in the temperature, and consequently

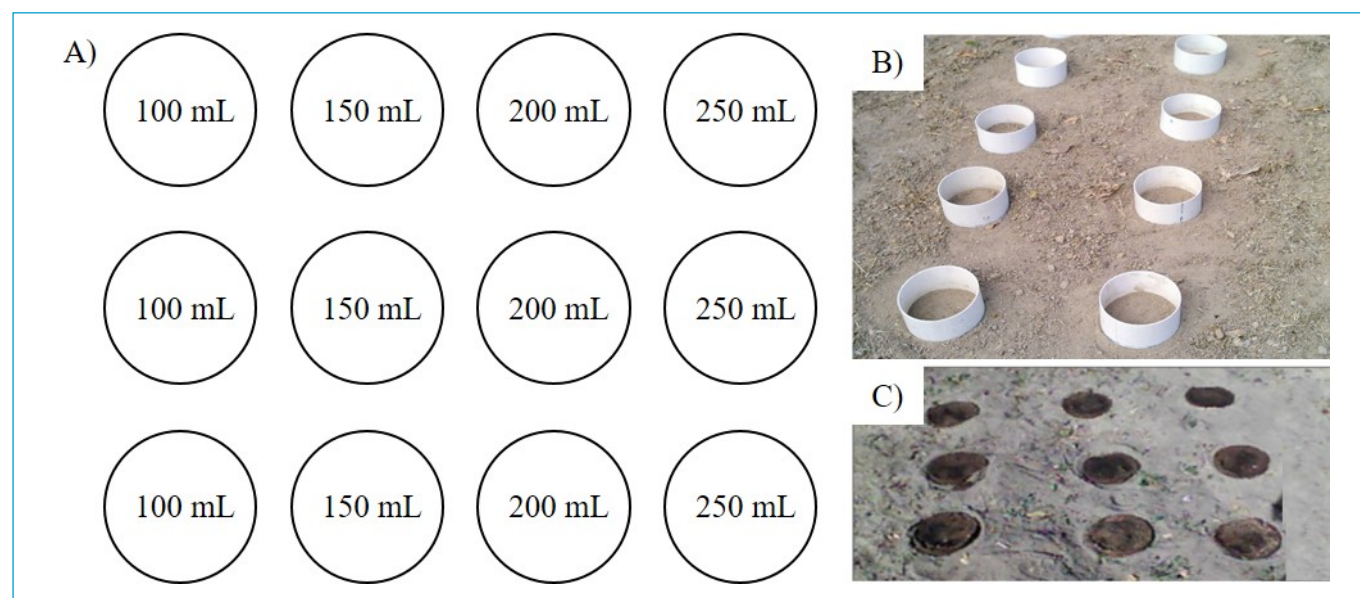


**Figure 2** – (A) Schematic representation of the position of the polyvinyl chloride rings and applied volumes of water (100, 150, 200, 250, and 250 mL). (B) Photograph of the polyvinyl chloride rings inserted in the soil surface. (C) Photograph of the soil surface immediately after application of different water volumes and removal of the polyvinyl chloride rings.

in soil moisture, resulting from differences in applied water volumes. For each thermal register, temperature data were converted into soil moisture data using linear regressions comparing the volumetric soil moisture of the collected soil samples with the corresponding average temperature observed in the thermograms.

Soil moisture data obtained with the infrared thermographic technique were compared with the measured volumetric soil moisture by means of statistical indexes and regression analyses. The goodness of fit of soil surface permeability data was evaluated based on the coefficient of correlation ( $r$ ) and on the root mean square error (RMSE), which is calculated as follows (Equations 1 and 2):

$$r = \frac{\sum_{i=1}^N ((\theta_{obs_i} - \bar{\theta}_{obs}) \times (\theta_{sim_i} - \bar{\theta}_{sim}))}{\sqrt{\sum_{i=1}^N (\theta_{obs_i} - \bar{\theta}_{obs})^2 \times \sum_{i=1}^N (\theta_{sim_i} - \bar{\theta}_{sim})^2}} \quad (1)$$

$$RMSE = \sqrt{\frac{1}{N} \sum_{i=1}^N (\theta_{obs_i} - \theta_{sim_i})^2} \quad (2)$$

where  $\theta_{obs_i}$  is the observed soil moisture content (volumetric moisture collected at 0 – 0.05 m layer) at point  $i$ ,  $\theta_{sim_i}$  is the simulated moisture content (obtained using thermography) at point  $i$ ,  $\bar{\theta}_{obs}$  and  $\bar{\theta}_{sim}$  are the average moisture contents measured and simulated, and  $N$  is the number of data points.

### Unsaturated hydraulic conductivity

Unsaturated hydraulic conductivity of the two tested soils and the four applied water volumes was estimated using the van Genuchten-Mualem model (Equation 3) (MUALEM, 1976; VAN GENUCHTEN, 1980):

$$K(\theta) = K_s \left( \frac{\theta - \theta_r}{\theta_s - \theta_r} \right)^{1/2} \left\{ 1 - \left[ 1 - \left( \frac{\theta - \theta_r}{\theta_s - \theta_r} \right)^{1/m} \right]^m \right\}^2 \quad (3)$$

where  $K(\theta)$  ( $m \cdot s^{-1}$ ) is the hydraulic conductivity,  $K_s$  ( $m \cdot s^{-1}$ ) is the saturated hydraulic conductivity,  $\theta$  ( $m^3 m^{-3}$ ) is the soil water content,  $\theta_r$  and  $\theta_s$  ( $m^3 m^{-3}$ ) are the soil residual and saturated water contents, and  $m$  (-) is an empirical parameter of the model and depends on the soil type.  $\theta_r$ ,  $\theta_s$ , and  $m$  are defined from previous studies conducted in the same study area, in the Argisol (SILVA *et al.*, 2012) and Neossol (SILVA *et al.*, 2014), as follows: 0.026  $m^3 m^{-3}$ , 0.364  $m^3 m^{-3}$ , and 0.435 for the Argisol and 0.033  $m^3 m^{-3}$ , 0.331  $m^3 m^{-3}$ , and 0.152 for the Neossol.

The saturated hydraulic conductivity of the two soils was estimated using the Beerkan simplified method (Equation 4) (BAGARELLO *et al.*, 2012):

$$K_s = \frac{b}{0.467 \left( \frac{2.92}{r \alpha} + 1 \right)} \quad (4)$$

Where:  $r$  (m) is the radius of the ring and  $\alpha$  is an empirical parameter adopted as  $1.200 \times 10^{-5} m^{-1}$ , for being representative of the studied soil types (REYNOLDS; ELRICK, 2002a, 2002b);  $b$  ( $m \cdot s^{-1}$ ) is the slope of the linearized cumulative infiltration curve, estimated by a linear regression analysis of the  $i/\sqrt{t}$  data versus  $\sqrt{t}$  data, where  $i$  ( $m \cdot s^{-1}$ ) is infiltration rate and  $t$  (s) is time, estimated from the experiments as  $3.965 \times 10^{-5}$  and  $8.017 \times 10^{-5} m \cdot s^{-1}$ , for the Argisol and Neossol, respectively, according to Silva *et al.* (2012).

## RESULTS AND DISCUSSION

Thermograms of the soil surface after application of four different volumes of cold water (between 10 and 15°C) in initial hotter soils (64.3°C for Argisol and 66.4°C for Neossol) are shown in Figure 3, for both the Argisol and Neossol. In the thermograms, the delimitation of the wetted areas is clearly perceptible. The thermograms allow us to identify the tests where more water was applied to the soil surface, perceptible by the darker coloration, which is the result of lower temperatures. This happened because more cold water flowed into the initially warmer soil, diminishing temperature and generating higher soil moisture. Similar results were found by Abrantes *et al.* (2017) and de Lima *et al.* (2014).

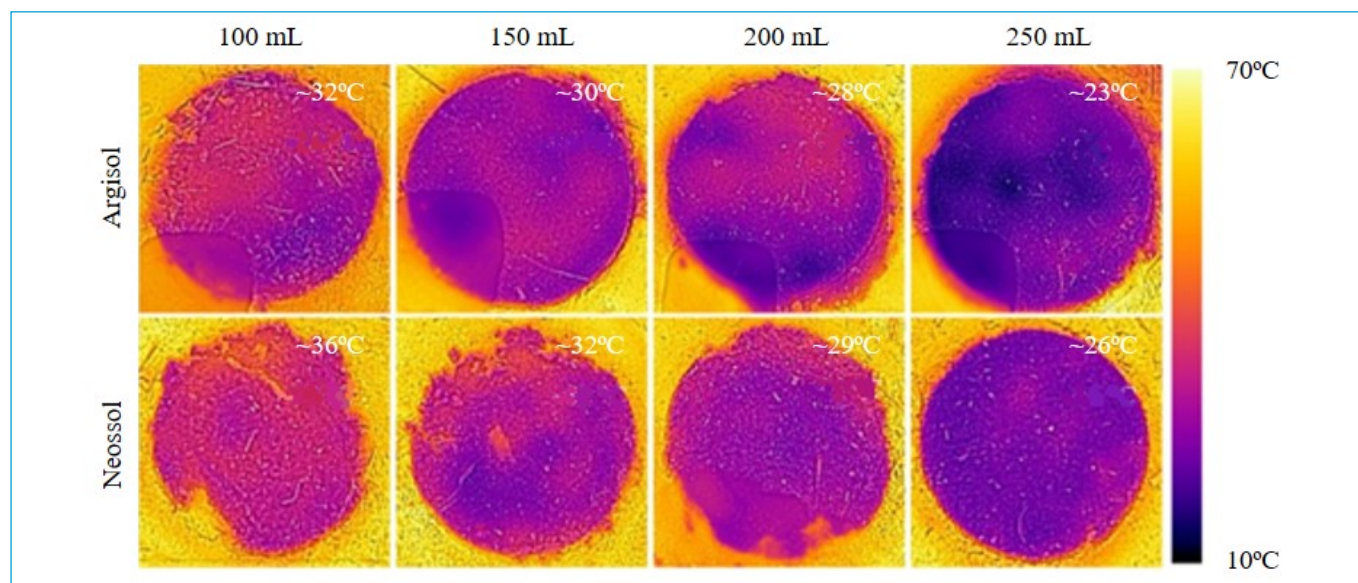


Figure 3 - Thermograms of the soil surface observed for both soils and applied water volumes, with respective average temperature.

When comparing the two soil types, it can be observed that, for the same applied water volumes, soil surface temperatures were very similar, despite the differences in the saturated hydraulic conductivity of  $3.720 \times 10^{-5}$  and  $5.000 \times 10^{-5} \text{ m}\cdot\text{s}^{-1}$  of the Argisol and Neossol, respectively (values calculated according to Equation 4). In fact, the highly permeable Neossol presented slightly higher temperatures because soil surface started to heat earlier after faster infiltration of water. However, these small differences between the two soils can also be attributed to small differences in initial soil temperatures (i.e., before cold water application).

Figure 4 presents a comparison between optical and thermal images of the same spot. The infrared thermographic technique allows us to clearly identify areas of different soil moisture that cannot be visually perceptible in the optical images. At last, only the delimitation caused by the ring insertion is visible.

A comparison between the four applied water volumes and the respective volumetric soil moisture measure through soil sampling is shown in Figure 5, for both the Argisol and Neossol. Here, the initial soil moisture (i.e., no applied water) was also plotted. The higher permeable Neossol presents slightly higher values of soil moisture than the Argisol. Soil moisture presented an approximately linear relation with the applied water volume, with determination coefficients ( $r^2$ ) higher than 0.9 for both soils. It should be noted that the linear relations presented in Figure 5 indicate only the general behavior of the data and the patterns of variations, as the values are case-dependent (e.g., soil characteristics and water and soil temperature).

A comparison between soil moisture and average soil surface temperature (obtained directly from the thermograms) of the wetted areas, after application of the different water volumes, is shown in Figure 6. For both soils and for all experiments, soil moisture presented an approximate inverse-exponential relation with soil surface temperature. For the morning experiments (hot water applied on initially cold soil), soil moisture increases with soil surface temperature, due to higher volume of applied hot water. On the contrary, for the afternoon experiments (cold water on initially hot soil), soil surface temperature decreases with increasing soil moisture, due to higher volumes of cold water. It is worth mentioning that the relation between soil moisture and average soil

surface temperature is case-dependent, and, therefore, the exponential relations only indicate trends.

Figure 7 shows the comparison between volumetric soil moisture obtained through soil sampling and using infrared thermography, across the wetted areas, for the Argisol and Neossol at initial soil surface temperatures of 61.9 and 67.2°C, respectively. Infrared thermography soil moisture values were obtained converting soil surface temperature values extracted from the thermograms using the regressions presented in Figure 6. For the Neossol, simulated soil moisture (using the infrared technique) overestimated the measured soil moisture for the 100 mL and underestimated for the 150 mL, probably due to natural intrinsic variability, sampling errors, and simplifications of the regression model. Moreover, lower volumes of applied water might produce non-uniform wetting of soil surface and lateral water movements in the rings, mainly for sandier soils, such as the Neossol. However, for higher volumes, the thermographic technique successfully represented the pattern. Similar behavior was also found by de Lima *et al.* (2014b), investigating the hydraulic conductivity in laboratory experiments, using thermography.

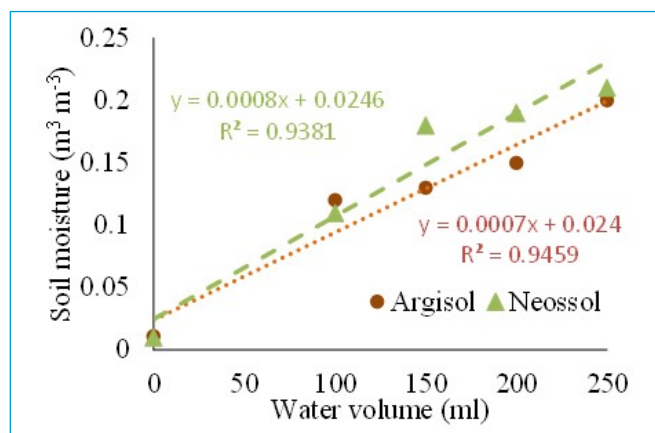


**Figure 5** - Correlation between the four volumes of water applied to the soil surface (100, 150, 200, and 250 mL) and the respective soil moisture, for the two tested soils. Equations and coefficient of determination of linear trendlines are shown.

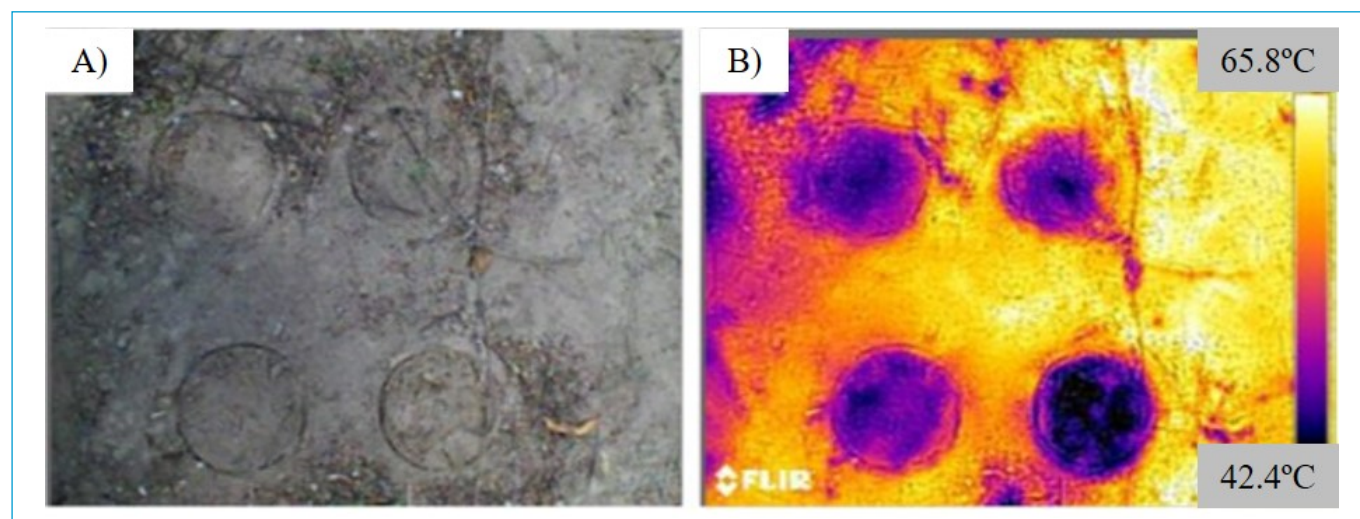


**Figure 4** - Example of an experiment performed in an Argisol, 5 min after application of the four water volumes. (A) Photograph of the soil surface without the visible presence of different soil moisture contents. (B) Thermal images of the soil surface with visible temperature differences as a result of differences in soil moisture.

It can be seen that the sharp variation of topsoil moisture, artificially created on the soil flume using the PVC rings, were not always represented by the thermography technique. This smoothing effect could be caused by the diffusion

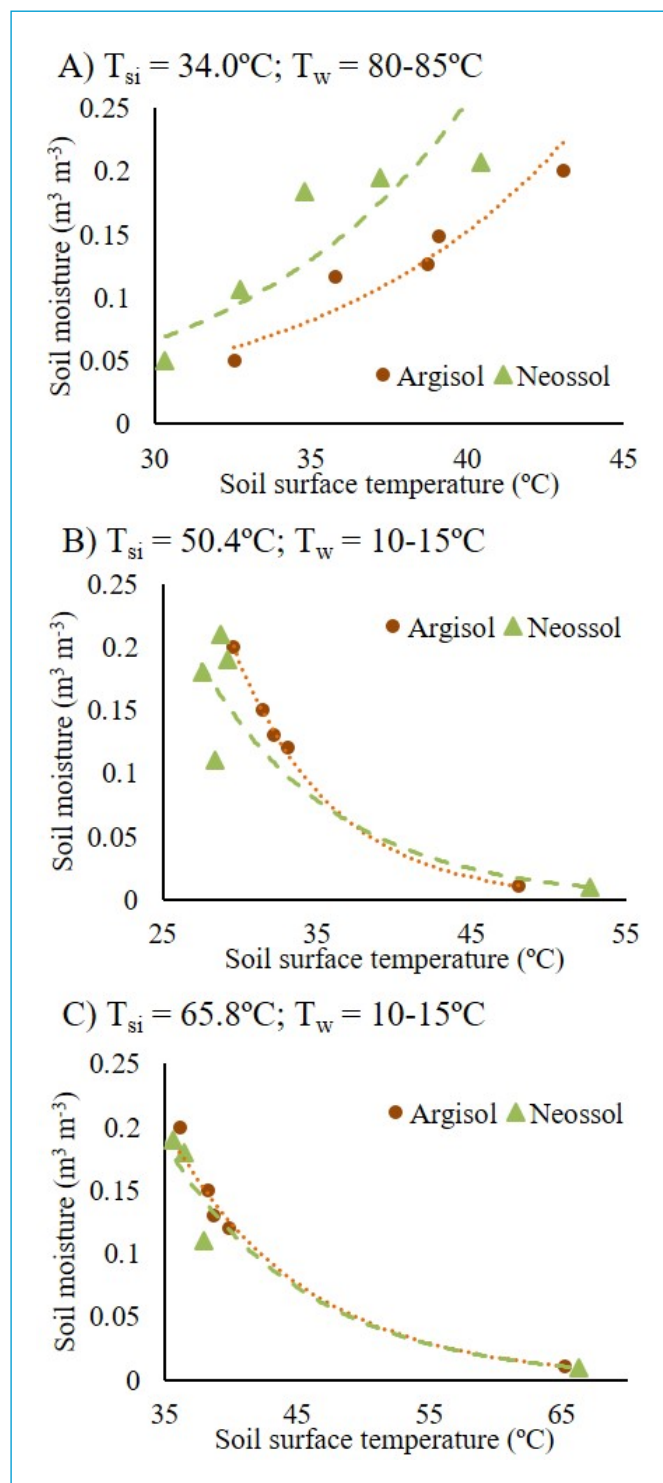


**Figure 6** - Comparison between soil moisture and soil temperature, for the different initial soil temperatures ( $T_{si}$ ) and applied water temperatures ( $T_w$ ). (A) Morning experiments with initially colder soil and application of hot water. (B) Afternoon experiments with initially hotter soil and application of cold water under the tree canopy. (C) Afternoon experiments with initially hotter soil and application of cold water under direct sunlight. Equations and coefficient of determination of exponential trendlines are shown.

of heat in those areas, which was also observed by Abrantes *et al.* (2017), de Lima and Abrantes (2014a), and de Lima *et al.* (2014).

Coefficient of correlation ( $r$ ) and RMSE for the different tests are presented in Table 1. For both soils, the technique was more successful in representing the soil moisture in the afternoon experiments with an initial soil temperature of above 60°C and water temperature between 10 and 15°C, with the highest  $r$ , always above 0.9, and lowest RMSE. This could be related to the higher difference of 55°C between the water and the soil surface, verified in these experiments. Nevertheless, in general, the technique successfully estimated soil moisture in all experiments with  $r$  values always higher than 0.7 and low RMSE values.

Figure 8 presents the curves of unsaturated hydraulic conductivity for both Argisol and Neossol, obtained from Equation 3. The saturated hydraulic conductivity used in Equation 3 was obtained using the simplified Beerkan method (Equation 4) (BRAUD *et al.*, 2005; LASSABATÈRE *et al.*, 2006; BAGARELLO *et al.*, 2012).

Using the curves presented in Figure 8, soil moisture values obtained with infrared thermography for the Argisol and Neossol (Figure 7) were converted to unsaturated hydraulic values and shown in Figure 9. The technique allowed us to map the spatial distribution of the topsoil surface conductivity for the different applied water volumes for both studied soils. Values of hydraulic conductivity indirectly obtained from the thermographic technique adequately represented the mean experimental *in situ* values measured by Silva *et al.* (2012), mainly for water volumes higher than 200 mL, for the Neossol.

### CONCLUSION

The technique presented in this study can be specifically useful to analyze qualitative real-time mapping of topsoil surface moisture spatial variability and identify areas of high and low soil moisture in a fast and expeditious way.

The technique can give a rough estimation of the spatial variability of unsaturated hydraulic conductivity of the topsoil and identify areas with similar permeability. These rough estimations can be used to complement observations from other techniques, therefore reducing the number of *in situ* random

**Table 1** - Correlation coefficient and root-mean-square error comparing soil moisture estimated through gravimetric soil sampling and estimated using infrared thermography, for the six experimental tests conducted for each soil type.

| Argisol        |      |      | Neossol       |      |      |
|----------------|------|------|---------------|------|------|
| Tw = 80 - 85°C |      |      |               |      |      |
| $T_{si}$ (°C)  | r    | RMSE | $T_{si}$ (°C) | r    | RMSE |
| 32.5           | 0.70 | 0.06 | 31.8          | 0.72 | 0.08 |
| 32.6           | 0.77 | 0.02 | 39.2          | 0.71 | 0.07 |
| Tw = 10 - 15°C |      |      |               |      |      |
| $T_{si}$ (°C)  | r    | RMSE | $T_{si}$ (°C) | r    | RMSE |
| 46.9           | 0.72 | 0.05 | 55.4          | 0.79 | 0.07 |
| 49.2           | 0.88 | 0.03 | 50.0          | 0.74 | 0.06 |
| 61.9           | 0.93 | 0.02 | 65.4          | 0.93 | 0.04 |
| 68.5           | 0.91 | 0.04 | 67.2          | 0.97 | 0.01 |

Tw: water temperature; Tsi: soil surface initial temperature, before water application; r: coefficient of correlation; RMSE: root-mean-square error.

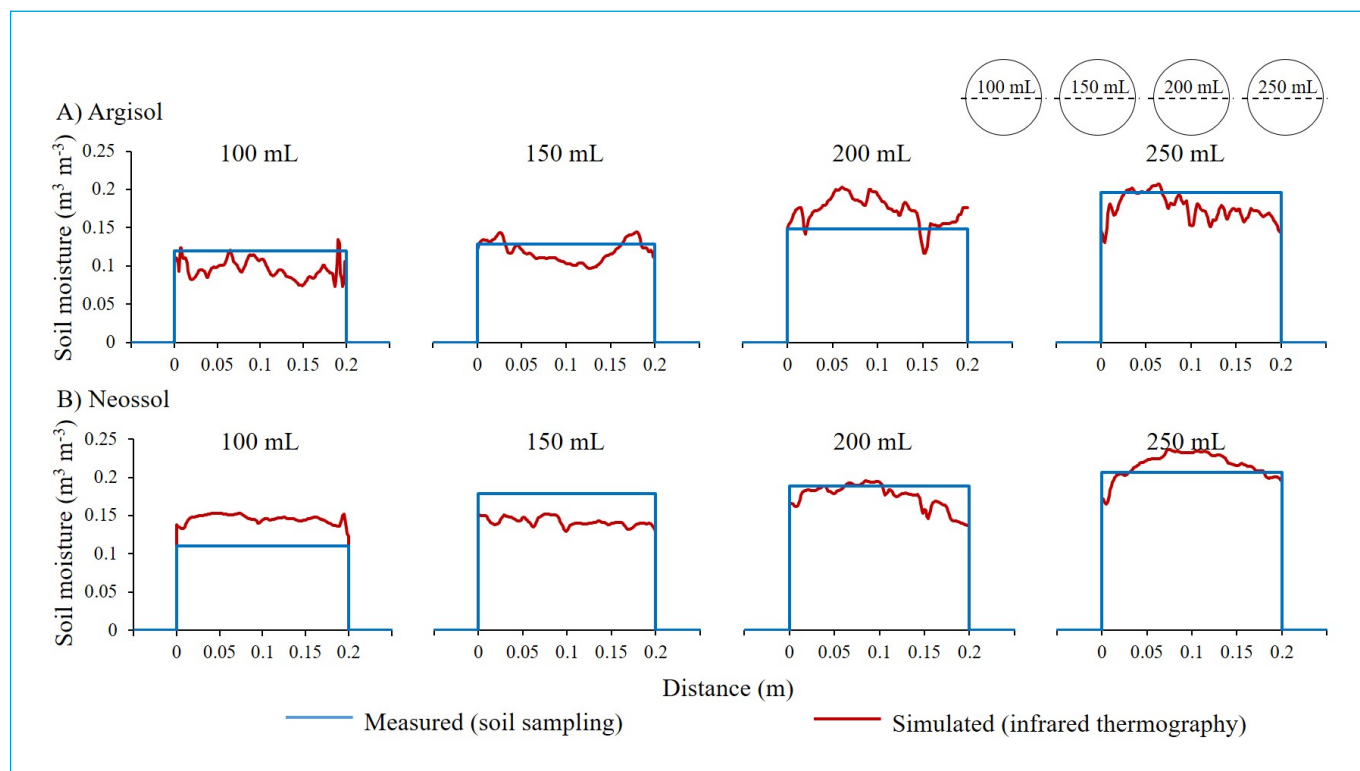


**Figure 7** - Comparison between soil moisture measured (gravimetric soil sampling-blue straight lines) and simulated with infrared thermography (red irregular lines), along cross-sections. (A) Argisol with an initial soil surface temperature of 61.9°C. (B) Neossol with an initial soil surface temperature of 67.2°C. Water temperature when applied was 10 - 15°C.

soil permeability tests (e.g., when using a double-ring infiltrometer), which are normally time-consuming techniques.

It should be noted that, when conducting experiences, higher differences between topsoil surface initial temperature and applied water give better results. In this study, experiments were limited to two soil types, and two distinct periods of the day, using temperatures of 10 - 15°C for the hot soil surfaces and 80 - 85°C for the cooler soil surfaces.

The following drawbacks of the proposed thermographic technique should also be noted: (i) the precision of the technique has to rely on *in situ* or laboratory reliable measurements of soil moisture (e.g., soil sampling and time-domain reflectometry (TDR) probes) needed for calibration and (ii) the technique should not be used to distinguish different topsoils, when testing environmental conditions are different (e.g., only when we have similar soil surface temperature, air temperature, wind speed, and humidity). As usual, a novel sensing tool will require thorough assessment to be routinely adopted in field monitoring practices and its development will require extensive calibration and validation.

## ACKNOWLEDGMENTS

The authors thank the Coordination for the Improvement of Higher Education Personnel (CAPES — Finance Code 001), the Foundation for the Support of Science and Technology of the State of Pernambuco (FACEPE — APQ-0300-5.03/17, APQ-0414-5.03/20 and IBPG-0855-5.03/20), the National Council for

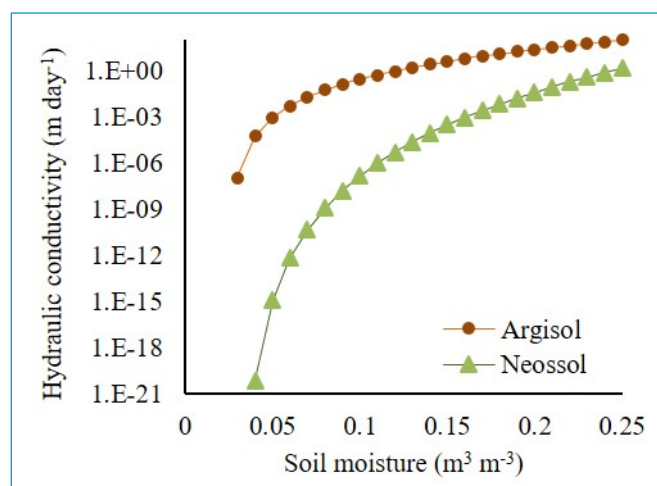


**Figure 8** - Hydraulic conductivity as a function of soil moisture, for the Argisol and Neossol.

Scientific and Technological Development (CNPq — 308.890/2018-3, 420.488/2018-9, 140281/2022-3), and the CAPES-PrInt/UFRPE for the financing of scholarships. This study had also the support of Portuguese funds through Foundation for Science and Technology, I. P (FCT), under the projects UIDB/04292/2020, UIDP/04292/2020, granted to MARE, and LA/P/0069/2020, granted to the Associate Laboratory ARNET.

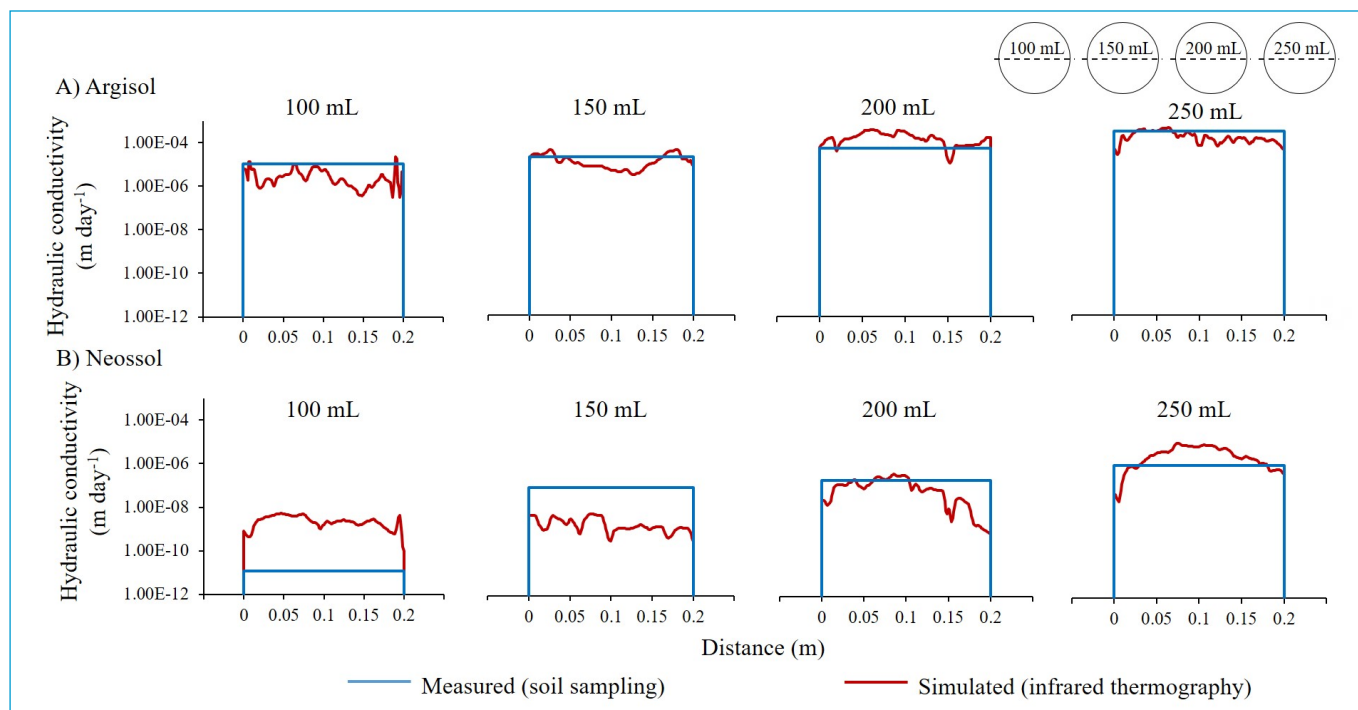


**Figure 9** – Comparison between hydraulic conductivity calculated from soil moisture data obtained on the basis of gravimetric soil sampling (blue straight lines) and simulated with infrared thermography (red curved lines), along cross-sections. (A) Argisol with an initial soil surface temperature of 61.9°C. (B) Neossol with an initial soil surface temperature of 67.2°C. Water temperature when applied was 10 - 15°C.

## AUTHORS' CONTRIBUTIONS

Montenegro, A.A.A.: Experimental procedures, Supervision, Data analysis, Discussion of results, General review. Lima, J. L. M. P.: Paper writing, Experimental design, Discussion of results, General review. Silva Junior, V. P.:

experimental measurements, data analysis, paper writing. Abrantes, J. R. C. B.: data analysis, results and discussion, paper writing. Silva, J. R. L.: Experimental measurements, Data analysis, Methodological conception.

## REFERÊNCIAS

- ABRANTES, J.R.C.B.; DE LIMA, J.L.M.P.; PRATS, S.A.; KEIZER, J.J. Assessing soil water repellency spatial variability using a thermographic technique: An exploratory study using a small-scale laboratory soil flume. *Geoderma*, v. 287, p. 98-104, 2017. <https://doi.org/10.1016/j.geoderma.2016.08.014>
- ABRANTES, J.R.C.B.; MORUZZI, R.B.; SILVEIRA, A.; DE LIMA, J.L.M.P. Comparison of thermal, salt and dye tracing to estimate shallow flow velocities: Novel triple tracer approach. *Journal of Hydrology*, v. 557, p. 362-377, 2018. <https://doi.org/10.1016/j.jhydrol.2017.12.048>
- ABRANTES, J.R.C.B.; MORUZZI, R.B.; DE LIMA, J.L.M.P.; SILVEIRA, A.; MONTENEGRO, A.A.A. Combining a thermal tracer with a transport model to estimate shallow flow velocities. *Physics and Chemistry of the Earth, Parts A/B/C*, v. 109, p. 59-69, 2019. <https://doi.org/10.1016/j.pce.2018.12.005>
- BAGARELLO, V.; DI, STEFANOC.; FERRO, V.; IOVINO, M.; SGROI, A. Physical and hydraulic characterization of a clay soil at the plot scale. *Journal of Hydrology*, v. 387, n. 1-4, p. 54-64, 2010. <https://doi.org/10.1016/j.jhydrol.2010.03.029>
- BAGARELLO, V.; DI, PRIMA.S.; IOVINO, M.; PROVENZANO, G. Estimating field-saturated soil hydraulic conductivity by a simplified Beerkan infiltration experiment. *Hydrological Processes*, v. 28, n. 3, p. 1095-1103, 2012. <https://doi.org/10.1002/hyp.9649>
- BONAR, S.A.; PETRE, S.J. Ground-based thermal imaging of stream surface temperatures: Technique and evaluation. *North American Journal of Fisheries Management*, v. 35, p. 1209-1218, 2015. <https://doi.org/10.1080/02755947.2015.1091410>
- BRAUD, I.; DE CONDAPPA, D.; SORIA, J.M.; HAVERKAMP, R.; ANGULO-JARAMILLO, R.; GALLE, S.; VAUCLIN, M. Use of scaled forms of the infiltration equation for the estimation of unsaturated soil hydraulic properties (the Beerkan method). *European Journal of Soil Science*, v. 56, p. 361-374, 2005. <https://doi.org/10.1111/j.1365-2389.2004.00660.x>
- CARVALHO, L.A.; LIBARDI, P.L.; ROCHA, G.C.; CRUZ, A.C.R. Hydraulic conductivity of a red Latosol (Rhodic ustox) associated to the soil profile pedologic characterization. *Ciência Rural*, v. 37, n. 4, p. 1008-1013, 2007. <https://doi.org/10.1590/S0103-84782007000400014>
- CHEN, X.; SONG, J.; CHENG, C.; WANG, D.; LACKEY, S.O. A new method for mapping variability in vertical seepage flux in streambeds.

- Hydrogeology Journal*, v. 17, p. 519-525, 2009. <https://doi.org/10.1007/s10040-008-0384-0>
- DE LIMA, J.L.M.P.; ABRANTES, J.R.C.B. Can infrared thermography be used to estimate soil surface microrelief and rill morphology? *Catena*, v. 113, p. 314-322, 2014a. <https://doi.org/10.1016/j.catena.2013.08.011>
- DE LIMA, J.L.M.P.; ABRANTES, J.R.C.B. Using a thermal tracer to estimate overland and rill flow velocities. *Earth Surface Processes and Landforms*, v. 39, p. 1293-1300, 2014b. <https://doi.org/10.1002/esp.3523>
- DE LIMA, J.L.M.P.; ABRANTES, J.R.C.B.; SILVA JR, V.P.; MONTENEGRO, A.A.A. Prediction of skin surface soil permeability by infrared thermography: a soil flume experiment. *Quantitative Infrared Thermography*, v. 11, p. 161-169, 2014. <https://doi.org/10.1080/17686733.2014.945325>
- DE LIMA, J.L.M.P.; SILVA JR, V.P.; DE LIMA, M.I.P.; ABRANTES, J.R.C.B.; MONTENEGRO, A.A.A. Revisiting simple methods to estimate drop size distributions: a novel approach based on infrared thermography. *Journal of Hydrology and Hydromechanics*, v. 63, n. 3, p. 220-227, 2015a. <https://doi.org/10.1515/johh-2015-0025>
- DE LIMA, J.L.M.P.; ZEHSAZ, S.; DE LIMA, M.I.P.; ISIDORO, J.M.G.P.; JORGE, R.G.; MARTINS, R. Using quinine as a fluorescent tracer to estimate overland flow velocities on bare soil: proof of concept under controlled laboratory conditions. *Agronomy*, v. 11, p. 1444, 2021. <https://doi.org/10.3390/agronomy11071444>
- DE LIMA, R.L.P.; ABRANTES, J.R.C.B.; DE LIMA, J.L.M.P.; DE LIMA, M.I.P. Using thermal tracers to estimate flow velocities of shallow flows: laboratory and field experiments. *Journal of Hydrology and Hydromechanics*, v. 63, p. 255-262, 2015b. <https://doi.org/10.1515/johh-2015-0028>
- EMPRESA BRASILEIRA DE PESQUISA AGROPECUÁRIA (EMBRAPA). *Manual de Métodos de Análises de Solo*. 2. ed. Rio de Janeiro: Ministério da Agricultura e do Abastecimento, 1997.
- GONÇALVES, A.D.M.A.; LIBARDI, P.L. An analysis of soil hydraulic conductivity determination by means of the instantaneous profile method. *Revista Brasileira de Ciência do Solo*, v. 37, n. 5, p. 1174-1184, 2013. <https://doi.org/10.1590/s0100-06832013000500007>
- HURTADO, A.L.B.; CICHOTA, R.; LIER, Q.J.V. Parameterization of the instantaneous profile method to determine soil hydraulic conductivity in evaporation experiments. *Revista Brasileira de Ciência do Solo*, v. 29, n. 2, p. 301-307, 2005. <https://doi.org/10.1590/s0100-06832005000200016>
- LASSABATÈRE, L.; ANGULO-JARAMILLO, R.; SORIA, U.J.M.; CUENCA, R.; BRAUD, I.; HAVERKAMP, R. Beerkan estimation of soil transfer parameters through infiltration experiments - BEST. *Soil Science Society American Journal*, v. 70, n. 2, p. 521-532, 2006. <https://doi.org/10.2136/sssaj2005.0026>
- MEJÍAS, M.; BALLESTEROS, B.J.; ANTÓN-PACHECO, C.; DOMÍNGUEZ, J.A.; GARCIA-ORELLANA, J.; GARCIA-SOLSONA, E.G.; MASQUÉ, P. Methodological study of submarine groundwater discharge from a karstic aquifer in the Western Mediterranean Sea. *Journal of Hydrology*, v. 464-465, p. 27-40, 2012. <https://doi.org/10.1016/j.jhydrol.2012.06.020>
- MUALEM, Y. A new model predicting the hydraulic conductivity of unsaturated porous media. *Water Resource Research*, v. 12, n. 3, p. 513-522, 1976. <https://doi.org/10.1029/WR012i003p00513>
- MUJTABA, B.; DE LIMA, J.L.M.P. Laboratory testing of a new thermal tracer for infrared-based PTV technique for shallow overland flows. *Catena*, v. 169, p. 69-79, 2018. <https://doi.org/10.1016/j.catena.2018.05.030>
- PFISTER, L.; MCDONNELL, J.J.; HISSLER, C.; HOFFMAN, L. Ground-based thermal imagery as a simple, practical tool for mapping saturated area connectivity and dynamics. *Hydrological Processes*, v. 24, n. 21, p. 3123-3132, 2010. <https://doi.org/10.1002/hyp.7840>
- REYNOLDS, W.D.; ELRICK, D.E. Principles and parameter definitions. In: DANE, J.H.; TOPP, G.C. (Eds.). *Methods of Soil Analysis: Part 1 - Physical Methods*. 3. ed. Madison, WI, SSSA, 2002a. p. 139-157.
- REYNOLDS, W.D.; ELRICK, D.E. Constant head well permeameter (vadose zone). In: DANE, J.H.; TOPP, G.C. (Eds.). *Methods of Soil Analysis: Part 1 - Physical Methods*. 3. ed. Madison, WI: SSSA, 2002b. p. 844-858.
- SCHUETZ, T.; WEILER, M.; LANGE, J.; STOELZLE, M. Two-dimensional assessment of solute transport in shallow waters with thermal imaging and heated water. *Advances in Water Resources*, v. 43, p. 67-75, 2012. <https://doi.org/10.1016/j.advwatres.2012.03.013>
- SILVA, J.R.L.; MONTENEGRO, A.A.A.; SANTOS, T.E.M. Hydraulic and physical characterization of soils in experimental basins of the Brazilian semiarid under conservation management. *Revista Brasileira de Engenharia Agrícola e Ambiental*, v. 16, n. 1, p. 27-36, 2012. <https://doi.org/10.1590/S1415-43662012000100004>
- SILVA, R.N.B.; LIMA J.R.S.; ANTONINO, A.C.D.; GONDIM, P.S.S.; SOUZA, E.S.; BARROS, J.R.G. Water balance in regosols cultivated with signal grass (*Brachiaria decumbens* Stapf). *Revista Brasileira de Ciência do Solo*, v. 38, n. 1, p. 147-157, 2014. <https://doi.org/10.1590/s0100-06832014000100014>
- TONOLLA, D.; ACUÑA, V.; UEHLINGER, U.; FRANK, T.; TOCKNER, K. Thermal heterogeneity in river floodplains. *Ecosystems*, v. 13, p. 727-740, 2010. <https://doi.org/10.1007/s10021-010-9350-5>
- VAN GENUCHTEN, M.T. A closed-form equation for predicting the hydraulic conductivity of unsaturated soils. *Soil Science Society American Journal*, v. 44, n. 5, p. 892-898, 1980. <https://doi.org/10.2136/sssaj1980.03615995004400050002x>
- VOORTMAN, B.R.; BOSVELD, F.C.; BARTHOLOMEUS, R.P.; WITTE, J.P.M. Spatial extrapolation of lysimeter results using thermal infrared imaging. *Journal of Hydrology*, v. 543, p. 230-241, 2016. <https://doi.org/10.1016/j.jhydrol.2016.09.064>